DOI: 10.1002/ejic.201100054

Preparation, Crystal Structures, Thermal Decomposition and Explosive Properties of Two Novel Energetic Compounds $M(IMI)_4(N_3)_2$ (M = Cu^{II} and Ni^{II}, IMI = Imidazole): The New High–Nitrogen Materials (N > 46%)

Bi-dong Wu,[a] Shi-wei Wang,[a] Li Yang,*[a] Tong-lai Zhang,[a] Jian-guo Zhang,[a] Zun-ning Zhou,[a] and Kai-bei Yu[a]

Keywords: Copper / Nickel / Azides / Imidazole / Decomposition / Sensitivity

Two novel multiligand coordination complexes of imidazole–copper(II) azide and imidazole–nickel(II) azide, $Cu(IMI)_4(N_3)_2$ and $Ni(IMI)_4(N_3)_2$, were synthesized and characterized by elemental analysis and FTIR spectroscopy. The crystal structures were determined by single-crystal X-ray diffraction. The results show that the crystals of $Cu(IMI)_4(N_3)_2$ and $Ni(IMI)_4(N_3)_2$ crystallize in the orthorhombic $Pna2_1$ and monoclinic $P2_1/n$ space groups, respectively. The metal cations are six-coordinate, and are bound to two azido ligands by μ_1-azido bridges and to four imidazole molecules through nitrogen atoms. Under nitrogen, with a heating rate of 5 K min^{-1}, these compounds go through two main exothermic stages between 420 K and 750 K during their thermal decompostion, as seen in the differential scanning calorimetry (DSC) and thermogravimetry–differential thermogravimetry (TG-DTG) curves. The nonisothermal kinetic parameters were calculated by the Kissinger and Ozawa methods. The sensitivity properties of $M(IMI)_4(N_3)_2$ were also determined by standard methods, and the results showed that $Cu(IMI)_4(N_3)_2$ had high impact and friction sensitivities and low flame sensitivity. $Ni(IMI)_4(N_3)_2$ had low sensitivity to external stimuli, but it had a very high energy of combustion. The results of all the studies showed that these $M(IMI)_4(N_3)_2$ (M = Cu^{II} and Ni^{II}) compounds have potential application as energetic materials.

Introduction

Energetic materials chemists have been interested in environmentally compatible green energetic materials, and this research field has proven to be fertile. In order to meet the requirements of future civil and military applications it is imperative to develop new energetic materials that have good thermal stability, mechanical insensitivity, good performance, with economic and environmentally friendly synthesis processes.[1,2] Therefore, a number of novel high-energy-density materials (HEDM) have been synthesized in recent years, and they have been suggested as suitable candidates for a range of applications including explosives, pyrotechnics, propellant formulations, and so forth.

Five-membered nitrogen-rich heterocyclic compounds are traditionally sources of energetic materials.[3–23] Imidazole (IMI) is a pentacyclic heterocyclic compound containing two nitrogen atoms and three carbon atoms and has a relatively small volume that may reduce steric hindrance and increase the material density. The functional group is –N=C–C=N–, and the key feature of these heterocycles is their π-electron configuration. Moreover, the role of the imidazole ring as a ligand is well known, and it has two potential N coordination sites that enable it to form extended structures, and its role as a ligand in a variety of coordination compounds has been well documented.[24–43] Many IMI derivatives have been studied in recent years such as 2-azidoimidazole,[24] imidazole-4-acetic acid,[25] 1,4-dinitroimidazole,[26] 2,4-dinitroimidazole,[27] 4,5-nitroimidazole,[28] 2,4,5-trinitroimidazole,[29] 1-methyl-2,4,5-trinitroimidazole (MTNI),[30] 2,4,5-tri(4-pyridyl)imidazole,[31] 1,2,4,5-tetranitroimidazole,[32] 4,4′,5,5′-tetranitro-2,2′-bi-1*H*-imidazole (TNBI)[34–35] and so on.[36–43] IMI and IMI derivative complexes are widely used in energetic materials, agriculture, medicine and other fields. In particular, studies of the coordination properties of IMI and its derivatives are of interest. For example, Tufan et al.[44] have reported four new clathrates with the general formula $M(IMI)_2Ni(CN)_4 \cdot 2C_6H_{12}$ (M = Mn^{II}, Co^{II}, Ni^{II} and Cd^{II}) and characterized them by IR and Raman spectroscopy. Their spectral results suggested that these compounds belong to the Hofmann type of clathrates. In 2009, Yazicilar et al.[45] reported four novel transition metal benzenesulfonate (BS) complexes of imidazole with general formulae $[M(IMI)_3(H_2O)_3]\cdot(BS)_2$ [M = Mn^{II}, Ni^{II} and Co^{II}] and $[Cu(BS)(IMI)_3]\cdot(BS)$. The results showed that these complexes exhibit different decomposition characteristics. Magnetic susceptibility measurements showed that the Co^{II} complex had orbital interactions. In

[a] State Key Laboratory of Explosion Science and Technology, Beijing Institute of Technology,
Beijing 100081, China
Fax: +86-10-68-911-202
E-mail: yanglibit@bit.edu.cn

Supporting information for this article is available on the WWW under http://dx.doi.org/10.1002/ejic.201100054.

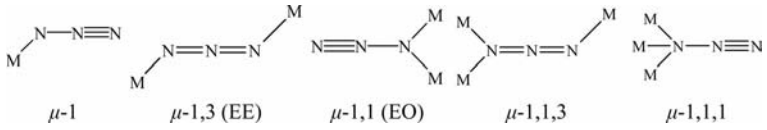

Figure 1. Different azido ligand coordination modes.

2010, Tong et al.[46] reported a density functional theory (DFT) study of [Mo$_2$O$_6$(IMI)$_4$]. The introduction of the IMI ligand into this complex resulted in a significant weakening of the important Mo–ligand interactions.

Researchers have also paid intense attention to the azido ligand due to its various coordination modes[47–51] (Figure 1). The various intriguing structures of azido–metal complexes, ranging from discrete structures to three-dimensional arrays, have promoted the development of coordination chemistry. Moreover, the azido ion has been studied due to its explosive nature, its ability to form pure and mixed-ligand complexes, its ambidentate nature and bridging capacity, and so on. In particular, azide coordination compounds have moderate thermal stability. Consequently, many scientists have performed considerable research on energetic azide coordination compounds. This can be demonstrated by consideration of some examples: Patil et al.[52] and Narang et al.[53] have systemically studied the synthesis of hydrazine–transition-metal azides by different methods that were developed between 1980 and 2000. At the beginning of the 21st century, Bose et al.[54] reported the synthesis, characterization, and single-crystal XRD analyses of [Zn(dpa)(N$_3$)$_2$] and [Zn(dpa)(N$_3$)(NO$_3$)]$_2$ (dpa = 2,2′-dipyridylamine), and discussed the role of dpa in crystal engineering and in the luminescence behavior of these compounds. Das et al.[55] have studied two new series of Zn^{II} complexes containing imidazole derivatives and N_3^- groups. Zhu et al.[56] have reported the optimization of the synthetic method for, and the explosive properties of, hydrazine–nickel(II) azide. They testified that this material is a potentially powerful primary explosive that possesses high flame sensitivity. Our research group have studied the synthesis, thermal decomposition, and explosive properties of energetic complexes [Cd$_2$(N$_2$H$_4$)$_2$(N$_3$)$_4$]$_n$,[57] Mn(CHZ)$_2$(N$_3$)$_2$[58] and [Cd(en)(N$_3$)$_2$]$_n$,[59] and have found that [Cd(en)(N$_3$)$_2$]$_n$ has good impact, friction, and flame sensitivities, and that [Cd$_2$(N$_2$H$_4$)$_2$(N$_3$)$_4$]$_n$ and Mn(CHZ)$_2$(N$_3$)$_2$ have good impact sensitivity. Such azido compounds have potential application as energetic materials.

In order to further the studies of imidazole–metal azide complexes, in this contribution we report two novel multiligand coordination complexes, Cu(IMI)$_4$(N$_3$)$_2$ and Ni(IMI)$_4$(N$_3$)$_2$, which have been synthesized and their crystal structures, the thermal decomposition mechanisms, and sensitivity properties evaluated.

Results and Discussion

Vibrational Spectroscopy

To gain a good understanding of the properties of the IMI group, molecular-orbital and IR absorption-frequency analyses based on the optimized structure were carried out by B3LYP functional analyses with the 6-311++g(d,p) basis set. The optimized structure was characterized to be associated with a true local energy minimum on the potential energy surface without an imaginary frequency component. The highest occupied molecular orbitals (HOMOs) and lowest unoccupied molecule orbitals (LUMOs) of the IMI group are shown in Figure 2. In the HOMO, the C=N double bond of the azo group may form a large π-orbital. The delocalized bonding orbitals show that the IMI group has a strongly conjugated system.

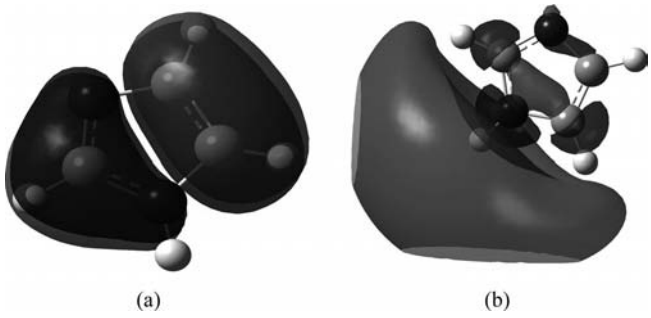

Figure 2. HOMO (a) and LUMO (b) of the IMI group.

The peaks in the calculated IR data can be assigned to four kinds of stretching and bending modes: symmetric and asymmetric stretching (υ_s, υ_{as}), in-plane bending (δ), out-of-plane bending (γ), and in-plane rocking (ω). The asymmetric N–C=N stretching mode of the ring and the C–N(=N) stretching mode of the azo group were observed. In the compounds, the ν_{as}(N–H) and ν_s(N–H) frequencies of the IMI group were shifted to lower wavenumbers than in the IMI spectrum because of the coordination effect of N_3^- with the central metal ion.

Molecule Structure

The structures of the compounds are shown in Figure 3, and selected bond lengths and angles of these compounds are listed in Tables 1 and 2.

From Figure 2, it can be seen that the electronic density of the HOMO at the N1 atom is relatively high. The formation of the coordination bond between the IMI N atom and the Cu^{II} or Ni^{II} ions is easy to understand, because the metal ions have unoccupied 3d orbitals. In the Cu(IMI)$_4$(N$_3$)$_2$ and Ni(IMI)$_4$(N$_3$)$_2$ molecules, there are single copper(II) and nickel(II) cations, respectively, and four imidazole molecules and two azido groups. The metal(II) cations contribute six empty orbitals to accommodate the lone-pair electrons of the ligands, that is to coordinate with the six N atoms of the four imidazole molecules and two

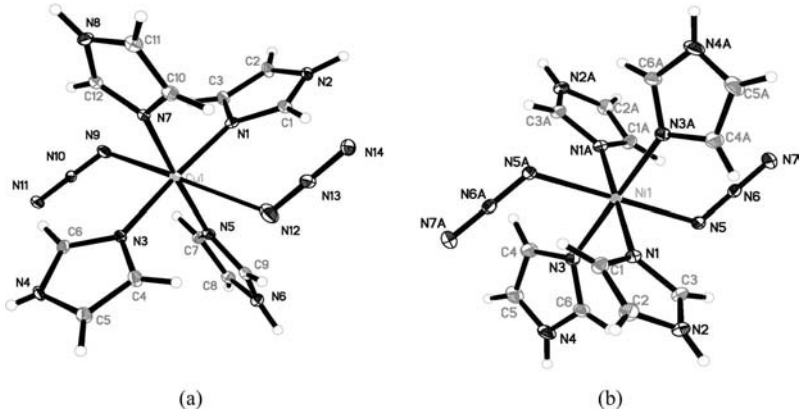

Figure 3. Molecular structures of $M(IMI)_4(N_3)_2$. (a) $Cu(IMI)_4(N_3)_2$, thermal ellipsoids drawn at 30% probability level; (b) $Ni(IMI)_4(N_3)_2$, thermal ellipsoids drawn at 10% probability level.

Table 1. Selected bond lengths [nm] and bond angles [°] for $Cu(IMI)_4(N_3)_2$.

Bond	[nm]	Bond	[nm]	Bond	[nm]
Cu1–N1	0.2017(3)	Cu1–N12	0.2846(4)	N2–H2	0.094(5)
Cu1–N3	0.2017(3)	N1–C3	0.1317(5)	N9–N10	0.1161(4)
Cu1–N5	0.2015(2)	N1–C1	0.1381(5)	N10–N11	0.1194(4)
Cu1–N7	0.2010(2)	N2–C3	0.1333(5)	N12–N13	0.1174(4)
Cu1–N9	0.2459(3)	N2–C2	0.1376(5)	N13–N14	0.1185(4)
Angle	[°]	Angle	[°]	Angle	[°]
N1–Cu1–N3	176.20(16)	N1–Cu1–N9	90.80(13)	N5–Cu1–N12	85.25(13)
N7–Cu1–N5	176.47(16)	N3–Cu1–N9	92.82(10)	N7–Cu1–N12	91.31(12)
N9–Cu1–N12	177.78(10)	N5–Cu1–N9	92.65(13)	N10–N9–Cu1	130.5(3)
N5–Cu1–N1	89.45(13)	N7–Cu1–N9	90.79(13)	N9–N10–N11	177.8(4)
N7–Cu1–N1	89.72(14)	N1–Cu1–N12	89.91(11)	N13–N12–Cu1	125.0(3)
N5–Cu1–N3	89.23(14)	N3–Cu1–N12	86.43(12)	N12–N13–N14	178.7(4)
N7–Cu1–N3	91.37(14)				

Table 2. Selected bond lengths [nm] and bond angles [°] for $Ni(IMI)_4(N_3)_2$.

Bond	[nm]	Bond	[nm]	Bond	[nm]
Ni1–N1	0.2092(2)	Ni1–N5A	0.2129(2)	N2–C2	0.1352(3)
Ni1–N1A	0.2092(2)	N5–N6	0.1178(2)	N2–C3	0.1331(3)
Ni1–N3	0.2121(2)	N6–N7	0.1161(2)	C1–C2	0.1346(3)
Ni1–N3A	0.2121(2)	N1–C1	0.1365(2)	N2–H2	0.083(2)
Ni1–N5	0.2129(2)	N1–C3	0.1318(2)		
Angle	[°]	Angle	[°]	Angle	[°]
N1A–Ni1–N1	180.00(8)	N6–N5–Ni1	121.39(13)	N1–Ni1–N5A	92.09(6)
N3A–Ni1–N3	180.00	N1–Ni1–N3	91.17(6)	N3–Ni1–N5	90.41(6)
N5A–Ni1–N5	180	N1–Ni1–N3A	88.83(6)	N3A–Ni1–N5	89.59(6)
N5–N6–N7	178.0(2)	N1–Ni1–N5	87.91(6)		

azido groups. The central metal(II) cations are coordinated to two azido groups that act as μ_1-bridging ligands [Cu–N bond lengths are 0.2459(3) and 0.2846(4) nm, and the Ni–N bond lengths are 0.2092(2) 0.2121(2) nm], and to four N atoms from imidazole ligands. Conforming to the general characteristics of coordinated azides, the μ_1-azido groups are nearly linear and asymmetric with <N9–N10–N11 177.8(4)°, N9–N10 0.1161(4) nm, N10–N11 0.1194(4) nm, <N12–N13–N14 178.7(4)°, N12–N13 0.1174(4) nm, N13–N14 0.1185(4) nm in the $Cu(IMI)_4(N_3)_2$ molecule, and <N5–N6–N7 178.0(2)°, N5–N6 0.1178(2) nm, N4–N5 0.1161(2) nm for the $Ni(IMI)_4(N_3)_2$ molecule.

In the $Cu(IMI)_4(N_3)_2$ molecule, the axial Cu–N bonds are ca. 0.04–0.08 nm longer than the four equivalent equatorial Cu–N bonds. This distorted lengthening of the bonds incorporating the Cu^{II} center can be attributed to the Jahn–Teller effect. The bond angles involving atoms N1 (N5) and N3 (N7) from two contraposition imidazole ligands and the copper(II) cation are <N1–Cu1–N3 176.20(16)° and <N5–Cu1–N7 176.47(16)°. The bond angles involving nitrogen atoms from two adjacent imidazole ligands and the copper(II) cation are <N1–Cu1–N5 89.45(13)°, <N1–Cu1–N7 89.72(14)°, <N7–Cu1–N9 90.79(13)° and <N5–Cu1–N12 85.25(13)°, all of which deviate from 90°. The distances be-

tween the copper(II) cation and the nitrogen atoms of the imidazole ligands are approximately equal [the Cu–N bond lengths are between 0.2010(2) and 0.2017(3) nm]. Therefore, the four nitrogen atoms of the imidazole ligands and the copper(II) cation exhibit a slightly distorted square configuration; the equation for the plane of these atoms (denoted plane A) is $-0.983x - 7.099y - 8.663z = -0.3851$. The distances between atoms N9, N12 from two azido groups and plane A are 0.2453 and 0.2831 nm, respectively. All the above data demonstrate that the Cu^{II} cation exhibits a slightly distorted octahedral configuration. The equations for the four planes formed by the imidazole rings are as follows:

N1–C1–N2–C2–C3 (plane B): $13.894x + 0.001y - 1.175z = 5.0225$;

N3–C4–N4–C5–C6 (plane C): $13.687x - 1.196y + 1.917z = 5.5089$;

N5–C7–N6–C8–C9 (plane D): $0.019x + 8.850y + 5.912z = 6.8743$;

N7–C10–N8–C11–C12 (plane E): $0.784x + 6.414y + 9.427z = 7.4631$.

The angles between planes A and B, planes A and D, and planes B and D are 97.9°, 105.8° and 92.6°, respectively, which all deviate from 90°. Therefore, planes B and C as well as planes D and E are not superposed, and the angles between them are 16.1° and 21.8°, respectively.

In the $Ni(IMI)_4(N_3)_2$ molecule, the bond angles involving atoms N1 (N3) and N1A (N3A) from two contraposition imidazole ligands and the nickel(II) cation are both 180.00° [<N1–Ni1–N1A 180.00(8)°, <N3–Ni1–N3A 180.00°]. The bond angles involving nitrogen atoms from two adjacent imidazole ligands and the nickel(II) cation are <N1–Ni1–N3 91.17(6)° and <N1–Ni1–N3A 88.83(6)°, both of which deviate from 90°. The distances between the nickel(II) cation and the nitrogen atoms of the imidazole ligands are all equal [Ni–N 0.2129(2) nm]. Therefore, the four nitrogen atoms of the imidazole ligand and the nickel(II) cation exhibit a slightly distorted quadrilateral configuration. The six coordination atoms and the central nickel(II) cation form three planes with the following plane equations:

Ni1–N1–N3–N1A (plane F): $-2.011x - 0.057y + 10.754z = 4.3432$;

N1–C1–N2–C2–C3 (plane G): $8.106x + 3.956y - 2.885z = 4.5896$;

N3–C4–N4–C5–C6 (plane H): $-3.492x + 4.929y + 9.524z = 5.4744$.

The angles between planes F and G, planes F and H, and planes G and H are 98.6°, 31.3° and 97.9°, respectively, which all deviate from 90°. However, the face-to-face imidazole rings are coplanar. The distance between N5 from an azido group and plane F is 0.2129(2) nm. All the above data demonstrate that the Ni^{II} cation exhibits a slightly distorted octahedral configuration.

Weak N–H···N hydrogen bonds between the azido groups and the imidazole ligands occur between the molecules in the solid state, and it can be seen from the crystal packing diagrams of these complexes (see Supporting Information) that all of these intermolecular hydrogen bonds extend the structures to give 3D supermolecular structures, and make an important contributions towards enhancing the thermal stability of the complexes.

Thermal Decomposition

In order to investigate the thermal behaviors of the title compounds they were analyzed by DSC and TG-DTG, with a linear heating rate of 5 K min^{-1} in a flowing N_2 atmosphere (flow rate 20 mL min^{-1}). The data curves from these analyses are shown in Figures 4 and 5. There are two main exothermic stages observed between 420 K and 750 K in the DSC curves. In the TG-DTG curves there are two main

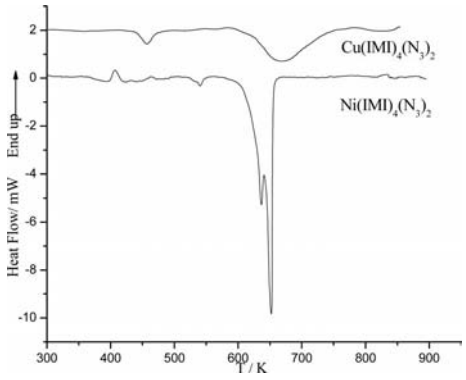

Figure 4. DSC curves of $M(IMI)_4(N_3)_2$ recorded in an N_2 atmosphere and with a heating rate of 5 K min^{-1}.

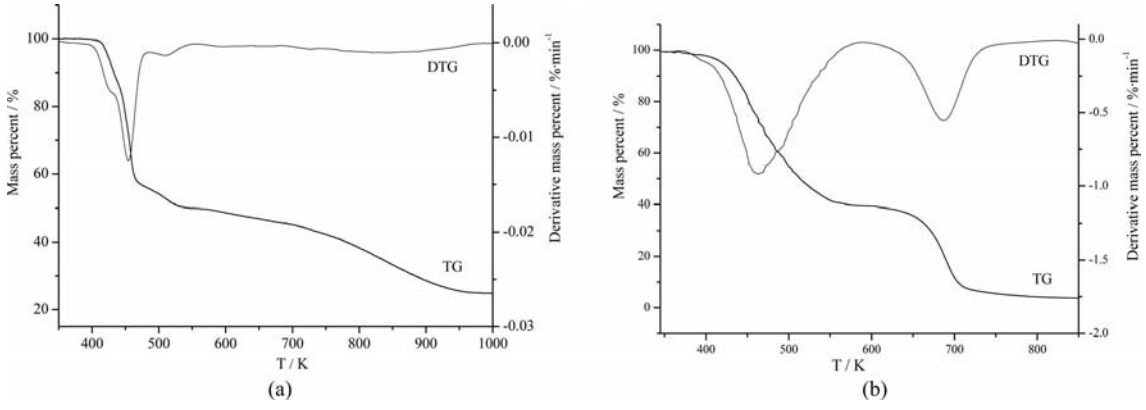

Figure 5. TG-DTG curves of $M(IMI)_4(N_3)_2$ recorded in an N_2 atmosphere and with a heating rate of 5 K min^{-1}. (a) $Cu(IMI)_4(N_3)_2$; (b) $Ni(IMI)_4(N_3)_2$.

successive mass losses that correspond to the successive exothermic stages seen in the DSC curves.

For the $Cu(IMI)_4(N_3)_2$ compound the melting point was not observed in the DSC curve. The exothermic stages were slow decomposition stages, and peaks were observed at 463 K and 671 K. The TG-DTG curves showed a mass loss of 50.67% in the first stage of decomposition that occurred over this temperature range, and reached the highest rate of mass loss at 455 K when the mass loss percentage equalled 15.14% min^{-1}. The second mass-loss stage occurred very slowly, and the total mass loss was 23.48%.

In the DSC curve of $Ni(IMI)_4(N_3)$ a melting point peak with a corresponding endothermic stage can be seen in the 420–450 K range. An exothermic slow decomposition stage is seen in the DCS data between 550 K and 565 K. The TG-DTG curve for this complex shows a mass loss of 60.68% in the first stage of decomposition over the 420–450 K temperature range, and reached the greatest rate of loss at 451 K with a mass-loss percentage of 6.82% min^{-1}. The main successive exothermic stages between 640 K and 690 K correspond to a decomposition stage. The corresponding TG-DTG curves show that the second mass loss was 36.42%, and reached the greatest rate of loss at 689 K with mass a loss percentage of 8.20%.

In order to study the energies of combustion and the enthalpies of formation of the title compounds, constant-volume energies of combustion (Q_v) for $Cu(IMI)_4(N_3)_2$ and $Ni(IMI)_4(N_3)_2$ were measured by oxygen bomb calorimetry, and were determined to be 11.09 MJ kg^{-1} and 16.71 MJ kg^{-1}, respectively. The bomb Equations (1) and (2) are as follows:

$$CuC_{12}H_{16}N_{14} + 16.5O_2 \rightarrow CuO + 8H_2O + 12CO_2 + 7N_2 \quad (1)$$

$$NiC_{12}H_{16}N_{14} + 16.5O_2 \rightarrow NiO + 8H_2O + 12CO_2 + 7N_2 \quad (2)$$

The energies of combustion are given by Equations (3) and (4):

$$\Delta H_{Cu(IMI)_4(N_3)_2} = Q_p = Q_v + \Delta nRT = 4683.05 \text{ kJ mol}^{-1} = 11.15 \text{ MJ kg}^{-1} \quad (3)$$

$$\Delta H_{Ni(IMI)_4(N_3)_2} = Q_p = Q_v + \Delta nRT = 6942.52 \text{ kJ mol}^{-1} = 16.73 \text{ MJ kg}^{-1} \quad (4)$$

The energies of combustion of cyclotrimethylenetrinitramine (RDX), cyclotetramethylenetetranitramine (HMX) and 2,4,6-trinitrotoluene (TNT) have been reported in the literature and are 9.60 MJ kg^{-1}, 9.44–9.88 MJ kg^{-1} and 15.22 MJ kg^{-1},[60] respectively. Therefore, the energy of combustion of $Cu(IMI)_4(N_3)_2$ is lower than that of TNT, yet the energy of combustion of $Ni(IMI)_4(N_3)_2$ is higher than that of RDX, HMX and TNT.

These two metal coordination complexes should be thermodynamically relatively stable structures. The standard enthalpies of formation of the $M(IMI)_4(N_3)_2$ complexes were back-calculated from the energies of combustion on the basis of Equations (1) and (2), and with Hess's Law as given in Equation (5). With the known enthalpies of formation of copper oxide $\{\Delta_fH°_{298}[CuO(s)] = -155.2 \text{ kJ mol}^{-1}\}$, nickel oxide $\{\Delta_fH°_{298}[NiO(s)] = -224.3 \text{ kJ mol}^{-1}\}$, carbon dioxide $\{\Delta_fH°_{298}[CO_2(g)] = 393.5 \text{ kJ mol}^{-1}\}$ and water $\{\Delta_fH°_{298}[H_2O(l)] = -285.8 \text{ kJ mol}^{-1}\}$, the enthalpies of formation of $Cu(IMI)_4(N_3)_2$ and $Ni(IMI)_4(N_3)_2$ can be calculated:

$$\Delta_fH°\{[M(IMI)_4(N_3)_2](s)\} = \Delta_fH°[MO(s)] + 8\Delta_fH°[H_2O(l)] + 12\Delta_fH°[CO_2(g)] - \Delta_cH°\{[M(IMI)_4(N_3)_2](s)\} \quad (5)$$

$\Delta_fH°_{298}\{[Cu(IMI)_4(N_3)_2](s)\} = -2402.6 \text{ kJ mol}^{-1}$;

$\Delta_fH°_{298}\{[Ni(IMI)_4(N_3)_2](s)\} = -4731.2 \text{ kJ mol}^{-1}$.

Non-Isothermal Kinetics Analysis

Kissinger's[61] and Ozawa's methods[62] are widely used to determine the Arrhenius equation for a given material. The Kissinger [Equation (6)] and Ozawa equations [Equation (7)] are as follows:

$$\ln\frac{\beta}{T_p^2} = \ln\left[\frac{RA}{E}\right] - \frac{E}{R}\cdot\frac{1}{T_p} \quad (6)$$

$$\lg\beta = \lg\frac{AE}{RG(\alpha)} - 2.315 - 0.4567\frac{E}{RT_p} \quad (7)$$

T_p is the temperature [K] at which the exothermic peak occurs in the DSC curve; A is the pre-exponential factor [s^{-1}]; E is the apparent activation energy [kJ mol^{-1}]; R is the gas constant (8.314 J K^{-1} mol^{-1}); β is the linear heating rate [K min^{-1}]; and $G(\alpha)$ is the reaction-mechanism function.

Based on the temperatures at which the first exothermic peaks occur in the DSC curves measured with four different heating rates (5, 10, 15 and 20 K min^{-1}), Kissinger's and Ozawa's methods were applied to study the kinetics parameters of the title compounds. From these data, the apparent activation energies E_K and E_O (E is the average value of E_K and E_O), pre-exponential factor A_K, linear correlation coefficients R_K and R_O, and standard deviations S_K and S_O were determined and are listed in Table 3.

Table 3. Temperatures of the first main exothermic peaks in the DSC curves of the compounds recorded at different heating rates, and chemical kinetics parameters for these complexes.

	$Cu(IMI)_4(N_3)_2$	$Ni(IMI)_4(N_3)_2$
T_p [K] values recorded with heating rates 5, 10, 15, 20 K min^{-1}	457.45, 462.75, 463.95, 465.75	637.35, 669.65, 690.05, 692.85
Kissinger's method		
E_K [kJ mol^{-1}], ln A_k, R_k, S_k	286.1, 30.79, –0.9852, 0.1229	73.9, 3.31, –0.9819, 0.1219
Ozawa's method		
E_O [kJ mol^{-1}], R_o, S_o	279.4, –0.986, 0.05338	80.8, –0.9861, 0.05316

Accordingly, the Arrhenius equations for the $M(IMI)_4(N_3)_2$ complexes can be expressed as Equations (8) and (9):

$$\ln k = 30.79 - 282.75 \times 10^3/(RT) \text{ for } Cu(IMI)_4(N_3)_2 \quad (8)$$

$$\ln k = 3.31 - 77.35 \times 10^3/(RT) \text{ for } Ni(IMI)_4(N_3)_2 \quad (9)$$

Sensitivity Tests

By applying the China National Military Standard, the impact, friction, and flame sensitivities of the complexes were determined.[63]

The impact sensitivities of the complexes were determined with a fall-hammer apparatus. A sample of $M(IMI)_4(N_3)_2$ (30 mg) was placed between two steel poles and hit with a 2.0 kg drop hammer from a starting height of 25 cm. The test results showed that the firing rate was 100%, and the 50% firing height (h_{50}) was 21.2 cm (4.16 J) for $Cu(IMI)_4(N_3)_2$. For $Ni(IMI)_4(N_3)_2$, h_{50} = 74.8 cm (14.7 J).

Friction sensitivities were determined with an MGY-1 pendular friction sensitivity apparatus by a standard procedure with 20 mg of sample. When $Cu(IMI)_4(N_3)_2$ was compressed between two steel poles with mirror surfaces at a pressure of 1.23 MPa and then hit with a 1.5 kg hammer at a 70° angle relative to the horizontal, the firing rate was 100%. Conversely, when $Ni(IMI)_4(N_3)_2$ was compressed at a pressure of 3.92 MPa and hit at a 90° angle relative to the horizontal, the firing rate was 48%.

Flame sensitivities were determined by a standard method in which the sample was ignited by a standard black powder pellet. $Cu(IMI)_4(N_3)_2$ and $Ni(IMI)_4(N_3)_2$ (20 mg) were compacted into a copper cap under a pressure of 58.8 MPa before being ignited by a standard black powder pellet. The test results showed that the 50% firing height (h_{50}) of $Cu(IMI)_4(N_3)_2$ was 13.94 cm, and that there was no fire at a minimum height of 6 cm for $Ni(IMI)_4(N_3)_2$.

Therefore, compared to hydrazine–nickel(II) azide,[56] $Cu(IMI)_4(N_3)_2$ has a very high sensitivity to external stimuli.

Physicochemical Properties

The physicochemical properties of the $M(IMI)_4(N_3)_2$ complexes are given in Table 4. These compounds are nitrogen-rich materials, with their nitrogen contents being higher than 46%. Furthermore, these compounds have lower oxygen balance values than TNT (Ω = –74.0%).

Table 4. Physicochemical properties of $M(IMI)_4(N_3)_2$ complexes.

	$Cu(IMI)_4(N_3)_2$	$Ni(IMI)_4(N_3)_2$
T_m [K][a]		407
T_d [K][b]	457; 666	637; 653
N [%][c]	46.70	47.27
Ω [%][d]	–125.74	–127.20
E [kJ mol^{-1}][e]	282.75	77.35
$\Delta H°$ [kJ mol^{-1}][f]	4683.1	6942.5
$\Delta_f H°_{298}$ [kJ mol^{-1}][g]	–2402.6	–4731.2
Impact sensitivity [J]	4.16	14.7

[a] Melting point/DSC endothermic peak. [b] Thermal degradation/DSC main exothermic peak. [c] Nitrogen content. [d] Oxygen balance. [e] Activation energy. [f] Experimental energy of combustion. [g] Molar enthalpy of formation.

Conclusions

Two novel high-nitrogen and environmental friendly energetic complexes of imidazole–copper(II) azide and imidazole–nickel(II) azide, $Cu(IMI)_4(N_3)_2$ and $Ni(IMI)_4(N_3)_2$, were synthesized and characterized. The crystal structures show that the Cu^{II} and Ni^{II} ions in these complexes are six-coordinate, have slightly distorted octahedral geometries, and are bound to two azido ligands in μ_1-modes and four imidazole molecules. The results from the thermal analysis of these compounds indicated that they undergo two main exothermic stages, as seen in the DSC and corresponding TG-DTG curves. The energies of combustion and the enthalpies of formation of $Cu(IMI)_4(N_3)_2$ and $Ni(IMI)_4(N_3)_2$ have been determined experimentally; the combustion energies for these copper and nickel complexes are 11.15 MJ kg^{-1} and 16.73 MJ kg^{-1}, respectively, and their enthalpies of formation are –2402.6 kJ mol^{-1} and –4731.2 kJ mol^{-1}, respectively. Non-isothermal kinetics analyses results indicated that the Arrhenius equation of $Cu(IMI)_4(N_3)_2$ and $Ni(IMI)_4(N_3)_2$ can be expressed as $\ln k = 30.79 - 282.75 \times 10^3/(RT)$ and $\ln k = 3.31 - 77.35 \times 10^3/(RT)$, respectively. The sensitivity measurement results for $Cu(IMI)_4(N_3)_2$ showed that the 50% firing heights for impact and flame sensitivities were 21.2 and 13.94 cm, respectively, and the friction sensitivity firing rate was 100% with a 1.5 kg hammer, 70° angle, and 1.23 MPa pressure. Therefore, $Cu(IMI)_4(N_3)_2$ has a good mechanical sensitivity and good combustion performance. Although $Ni(IMI)_4(N_3)_2$ has a lower sensitivity than the corresponding copper complex, it has a high heat of combustion that is higher than those of RDX, HMX and TNT. In other words, $Ni(IMI)_4(N_3)_2$ can be regarded as an energy additive that can be applied to improve the explosion performance of traditional explosives and propellant formulations. In conclusion, the results of these studies have shown that $M(IMI)_4(N_3)_2$ (M = Cu^{II} and Ni^{II}) complexes have potential application as energetic materials.

Experimental Section

Caution: The title compounds are energetic materials and tend to explode under certain conditions. Appropriate safety precautions (safety glasses, face shield, leather coat and ear plugs) should be taken, especially when these compounds are prepared on a large scale and in dry state.

Materials and Physical Techniques: The copper sulfate pentahydrate ($CuSO_4 \cdot 5H_2O$), nickel acetate hexahydrate [$Ni(OAc)_2 \cdot 6H_2O$] and imidazole reagents were all analytically pure commercial products. The starting material sodium azide was a commercial product that was purified by recrystallization prior to use. Elemental analyses were performed with a Flash EA 1112 fully automatic trace element analyzer. FTIR spectra were recorded with a Bruker Equinox 55 infrared spectrometer (KBr pellets) over the 4000–400 cm^{-1}

Table 5. Crystal data and structure refinement details for $M(IMI)_4(N_3)_2$ complexes.

	$Cu(IMI)_4(N_3)_2$	$Ni(IMI)_4(N_3)_2$
Empirical formula	$C_{12}H_{16}CuN_{14}$	$C_{12}H_{16}N_{14}Ni$
Formula mass	419.93	415.08
Crystal dimensions [mm]	$0.33 \times 0.27 \times 0.07$	$0.33 \times 0.23 \times 0.23$
Crystal system	orthorhombic	monoclinic
Space group	$Pna2_1$	$P2_1/n$
Z	4	2
a, b, c [nm]	1.3958(3), 1.0110(2), 1.2228(3)	0.8777(3), 1.0464(3), 1.0847(4)
β [°]	90	110.728(3)
h, k, l	–13 to 18, –13 to 13, –15 to 12	–10 to 11, –11 to 13, –14 to 14
Temperature [K]	93(2)	295(2)
Unit cell volume, V [nm^3]	1.7255(7)	0.9317(5)
D_c [g cm^{-3}]	1.616	1.480
λ [nm]	0.071073	0.071073
μ (Mo-K_α) [mm^{-1}]	1.299	1.072
F(000)	860	428
θ range [°]	3.33–27.47	3.15–27.45
Max., min. transmission	0.9146, 0.6716	0.7884, 0.7167
Measured reflections	13356	7072
Unique data	3600 (R_{int} = 0.0206)	2090 (R_{int} = 0.0267)
R_1, wR_2 [$I > 2\sigma(I)$]	R_1 = 0.0402, wR_2[a] = 0.0821	R_1 = 0.0332, wR_2[b] = 0.0654
R_1, wR_2 (all data)	R_1 = 0.0374, wR_2[a] = 0.0802	R_1 = 0.0459, wR_2[b] = 0.0713
Goodness of fit	1.001	0.998
δp_{max}, δp_{min} [e nm^{-3}]	419, –370	0.316, 259

[a] $w = 1/[\sigma 2(F_o^2) + (0.0346\,P)^2 + 1.6900\,P]$. [b] $w = 1/[\sigma 2(F_o^2) + (0.0269\,P)^2 + 0.3160\,P]$. $wR_2 = [\sum w(F_o^2 - F_c^2)^2/\sum w(F_o^2)]^{1/2}$, $P = (F_o^2 + 2F_c^2)/3$.

range with a resolution of 4 cm^{-1}. DSC and TG-DTG measurements were carried with a Pyris-1 differential scanning calorimeter and Pyris-1 thermogravimetric analyzer (Perkin–Elmer, USA) with the sample under a dry nitrogen atmosphere (flow rate = 20 mL min^{-1}). For the DSC andTGA analyses the crystalline samples were powdered and placed in aluminum and open platinum pans, respectively; the samples were then heated from 323 K to 873 K with a linear heating rate of 10 K min^{-1}. The combustion heats of the title compounds were measured by oxygen bomb calorimetry (Parr 6200, USA).

Synthesis of $Cu(IMI)_4(N_3)_2$ and $Ni(IMI)_4(N_3)_2$: A solution of $CuSO_4 \cdot 5H_2O$ (2.5 g, 10 mmol) or $Ni(OAc)_2 \cdot 6H_2O$ (2.8 g, 10 mmol) in deionized water (100 mL) was placed in a glass reactor with a thermo-water bath. The reaction solution was stirred with a mechanical agitator and heated to 60–70 °C. Imidazole (2.72 g, 40 mmol) and sodium azide (1.30 g, 20 mmol) dissolved in deionized water (50 mL) were added to the $CuSO_4$ or $Ni(OAc)_2$ aqueous solution with continuous stirring and with the reaction solution maintained at 60–70 °C over the course of 30 min. Then the solution was cooled to room temperature with stirring. The precipitate that formed was collected by filtration, washed with ethanol, and dried under vacuum in an explosion-proof water-bath dryer. The yield was 69.0% for $Cu(IMI)_4(N_3)_2$ and 72.0% for $Ni(IMI)_4(N_3)_2$. Single crystals suitable for XRD measurements were obtained by recrystallizing the products from this hydrothermal method from deionized water at room temperature over a period of 1 month.

Elemental Analyses: $Cu(IMI)_4(N_3)_2$ (419.93): calcd. C 34.32, H 3.84, N 46.70; found C 34.41, H 3.74, N 46.93. $Ni(IMI)_4(N_3)_2$ (415.08): calcd. C 34.72, H 3.89, N 47.27; found C 35.06, H 3.67, N 47.10. IR (KBr pellets): $Cu(IMI)_4(N_3)_2$: $\tilde{\nu}$ = 3571 [w, vs (NH)], 3310 [vs (υ NH)], 2091 [vs (υ_{as} N_3^-)], 1620 [s (δ NH)], 1291 [w (υ N_3^-)], 834 [w (δ imidazole)], 681 [w (δ N_3^-)]. $Ni(IMI)_4(N_3)_2$: $\tilde{\nu}$ = 3133 [vs (υ NH)], 2056 [vs (υ_{as} N_3^-)], 1539 [s (δ NH)], 1257 [w (υ N_3^-)], 819 [w (δ imidazole)], 624 [w (δ N_3^-)] cm^{-1}.

X-ray Data Collection and Structure Refinement: Blue crystals were chosen for XRD analysis. The XRD data collections were performed with a Rigaku AFC-10/Saturn 724$^+$ CCD detector diffractometer with graphite-monochromated Mo-K_α radiation (λ = 0.071073 nm) in multi-scan mode for $Cu(IMI)_4(N_3)_2$ and in ϕ-ω scan mode for $Ni(IMI)_4(N_3)_2$. The structures were solved by direct methods with SHELXS-97[64] and refined by full-matrix least-squares methods on F^2 with SHELXL-97.[65] All non-hydrogen atoms were located from the difference Fourier maps and subjected to anisotropic refinement. Detailed information concerning the crystallographic data collections and structures refinements is summarized in Table 5. CCDC-796440 [for $Cu(IMI)_4(N_3)_2$] and -796439 [for $Ni(IMI)_4(N_3)_2$] contain the supplementary crystallographic data for this paper. These data can be obtained free of charge from The Cambridge Crystallographic Data Centre via www.ccdc.cam.ac.uk/data_request/cif.

Supporting Information (see footnote on the first page of this article): Hydrogen bond lengths and bond angles, metal cations' octahedral coordination structures, and the coplanar structures and the packing of the unit cell of $M(IMI)_4(N_3)_2$.

Acknowledgments

The project was supported by the Science and Technology on Applied Physical Chemistry Laboratory (9140C3703051105), the State Key Laboratory of Explosion Science and Technology (No.YBKT10-05 and ZDKT10-01b) and the Program for New Century Excellent Talents in University (NCET-10-0051, CNET-09-0051).

[1] J. Giles, *Nature* **2004**, *427*, 580–581.
[2] X. F. Sua, X. L. Cheng, C. M. Meng, X. L. Yuan, *J. Hazard. Mater.* **2009**, *161*, 551–551

[3] Y. G. Huang, H. X. Gao, B. Twamley, J. M. Shreeve, *Eur. J. Inorg. Chem.* **2008**, 2560–2568.
[4] Y. H. Joo, J. M. Shreeve, *Org. Lett.* **2008**, *10*, 4665–4667.
[5] Y. H. Joo, B. Twamley, S. Garg, J. M. Shreeve, *Angew. Chem. Int. Ed.* **2008**, *47*, 6236–6239.
[6] T. Abe, G. H. Tao, Y. H. Joo, Y. Huang, J. M. Shreeve, B. Twamley, *Angew. Chem. Int. Ed.* **2008**, *47*, 7087–7090.
[7] T. M. Klapötke, C. M. Sabaté, *Z. Anorg. Allg. Chem.* **2009**, *635*, 1812–1822.
[8] K. Karaghiosoff, T. M. Klapötke, C. M. Sabaté, *Chem. Eur. J.* **2009**, *15*, 1164–1176.
[9] T. M. Klapötke, J. Stierstorfer, B. Weber, *Inorg. Chim. Acta* **2009**, *362*, 2311–2320.
[10] K. Karaghiosoff, T. M. Klapötke, C. M. Sabaté, *Eur. J. Inorg. Chem.* **2009**, 238–250.
[11] Y. H. Joo, J. M. Shreeve, *Inorg. Chem.* **2009**, *48*, 8431–8438.
[12] T. Abe, G. H. Tao, Y. H. Joo, R. W. Winter, G. L. Gard, J. M. Shreeve, *Chem. Eur. J.* **2009**, *15*, 9897–9904.
[13] Y. H. Joo, B. Twamley, J. M. Shreeve, *Chem. Eur. J.* **2009**, *15*, 9097–9104.
[14] T. Abe, Y. H. Joo, G. H. Tao, B. Twamley, J. M. Shreeve, *Chem. Eur. J.* **2009**, *15*, 4102–4110.
[15] G. H. Tao, B. Twamley, J. M. Shreeve, *Inorg. Chem.* **2009**, *48*, 9918–9923.
[16] Y. G. Huang, H. X. Gao, B. Twamley, J. M. Shreeve, *Chem. Eur. J.* **2009**, *15*, 917–923.
[17] Y. H. Joo, J. M. Shreeve, *J. Am. Chem. Soc.* **2010**, *132*,15081–15090.
[18] R. Damavarapu, T. M. Klapötke, J. Stierstorfer, K. R. Tarantik, *Propellants, Explos., Pyrotech.* **2010**, *35*, 395–406.
[19] T. M. Klapötke, H. Radies, J. Stierstorfer, K. R. Tarantik, G. Chen, A. Nagori, *Propellants, Explos., Pyrotech.* **2010**, *35*, 213–219.
[20] R. H. Wang, H. Y. Xu, Y. Guo, R. J. Sa, J. M. Shreeve, *J. Am. Chem. Soc.* **2010**, *132*,11904–11905.
[21] Y. Guo, G. H. Tao, Z. Zeng, H. X. Gao, D. A. Parrish, J. M. Shreeve, *Chem. Eur. J.* **2010**, *16*, 3753–3762.
[22] M. Göbel, K. Karaghiosoff, T. M. Klapötke, D. G. Piercey, J. Stierstorfer, *J. Am. Chem. Soc.* **2010**, *132*,17216–17226.
[23] Y. H. Joo, J. M. Shreeve, *Angew. Chem. Int. Ed.* **2010**, *49*, 7320–7323.
[24] J. Villarrasa, E. Melendez, *An. Quim.* **1974**, *7*, 966–969.
[25] S. Materazzi, E. Vasca, *Thermochim. Acta* **2001**, *373*, 7–11.
[26] S. Bulusu, R. Damavarapu, J. R. Autera, R. Behrens Jr., L. M. Minier, J. Villanueva, K. Jayasuriya, T. Axenrod, *J. Phys. Chem.* **1995**, *99*, 5009–5015.
[27] K. Bhaumik, K. G. Akamanchi, *J. Heterocycl. Chem.* **2004**, *41*, 51–55.
[28] G. C. Yang, H. J. Liu, D. L. Cao, *Chin. J. Energ. Mater.* **2006**, *14*, 349–351.
[29] X. F. Su, X. L. Cheng, S. H. Ge, *THEOCHEM* **2009**, *895*, 44–51.
[30] J. R. Cho, K. J. Kim, S. G. Cho, J. K. Kim, *Indian J. Heterocycl. Chem.* **2002**, *39*, 141–147.
[31] L. Wang, W. Gu, J. X. Deng, M. L. Liu, N. Xu, X. Liu, *Z. Anorg. Allg. Chem.* **2009**, *636*, 1124–1128.
[32] S. G. Cho, B. S. Park, J. R. Cho, *Propellants, Explos., Pyrotech.* **1999**, *24*, 343–348.
[33] S. G. Cho, J. R. Cho, E. M. Goh, J. K. Kim, R. Damavarapu, R. Surapaneni, *Propellants, Explos., Pyrotech.* **2005**, *30*, 445–449.
[34] S. G. Cho, E. M. Goh, J. R. Cho, J. K. Kim, *Propellants, Explos., Pyrotech.* **2006**, *31*, 33–37.
[35] K. León, A. M. Riverón, O. Arencibia, L. López-Cánovas, *Anal. Biochem.* **2010**, *402*, 96–98.
[36] M. J. Wójcik, J. Kwiendacz, M. Boczar, Ł. Boda, Y. Ozaki, *Chem. Phys.* **2010**, *372*, 72–81.
[37] W. H. Liu, A. B. Greytak, J. M. Lee, C. Wong, J. Park, L. F. Marshall, W. Jiang, P. N. Curtin, A. Y. Ting, D. G. Nocera, D. Fukumura, R. K. Jain, M. G. Bawendi, *J. Am. Chem. Soc.* **2010**, *132*, 472–483.
[38] C. J. Hu, C. D. Sulok, F. Paulat, N. Lehnert, A. I. Twigg, M. P. Hendrich, C. E. Schulz, W. R. Scheidt, *J. Am. Chem. Soc.* **2010**, *132*, 3737–3750.
[39] K. Kawamura, M. Naganawa, F. Konnoa, J. Yui, H. Wakizaka, T. Yamasaki, K. Yanamotoa, A. Hatori, M. Takei, Y. Yoshida, K. Sakaguchi, T. Fukumura, Y. Kimura, M. R. Zhang, *Nucl. Med. Biol.* **2010**, *37*, 625–635.
[40] L. Han, P. P. Zhang, H. S. Liu, H. J. Pang, Y. Chen, J. Peng, *J. Cluster Sci.* **2010**, *21*, 81–91.
[41] A. Pramanik, A. Basu, G. Das, *Polyhedron* **2010**, *29*, 1980–1989.
[42] H. Y. Bai, J. F. Ma, J. Yang, Y. Y. Liu, H. Wu, J. C. Ma, *Cryst. Growth Des.* **2010**, *10*, 995–1016.
[43] M. Fantini, V. Zuliani, M. A. Spotti, M. Rivara, *J. Comb. Chem.* **2010**, *12*, 181–185.
[44] Y. Tufan, N. Karacan, J. E. D. Davies, *Vib. Spectrosc.* **2000**, *23*, 51–55.
[45] T. K. Yazicilar, E. Y. Gürkan, I. Ucar, C. Kazak, *Trans.-Met. Chem.* **2009**, *34*, 669–676.
[46] Y. P. Tong, Y. W. Lin, *THEOCHEM* **2010**, *952*, 61–66.
[47] T. M. Klapötke, B. Krumm, M. Scherr, *J. Am. Chem. Soc.* **2009**, *131*,72–74.
[48] E. Q. Gao, S. Q. Bai, Y. F. Yue, Z. M. Wang, C. H. Yan, *Inorg. Chem.* **2003**, *42*, 3642–3649.
[49] F. C. Liu, Y. F. Zeng, J. R. Li, X. H. Bu, H. J. Zhang, J. Ribas, *Inorg. Chem.* **2005**, *44*, 7298–7300.
[50] H. H. Ko, J. H. Lim, H. C. Kim, C. S. Hong, *Inorg. Chem.* **2006**, *45*, 8847–8849.
[51] M. A. S. Goher, B. Bitschnau, B. Sodin, C. Gspan, F. A. Mautner, *J. Mol. Struct.* **2008**, *886*, 32–38.
[52] K. C. Patil, C. Nesamani, V. R. P. Verneker, *Synth. React. Inorg. Met.-Org. Chem.* **1982**, *12*, 383–395.
[53] K. K. Narang, M. K. Singh, K. B. Singh, R. A. Lal, *Synth. React. Inorg. Met.-Org. Chem.* **1996**, *26*, 573–589.
[54] D. Bose, S. H. Rahaman, G. Mostafa, R. D. B. Walsh, M. J. Zaworotko, B. K. Ghosh, *Polyhedron* **2004**, *23*, 545–552.
[55] D. Das, B. G. Chand, K. K. Sarker, J. Dinda, C. Sinha, *Polyhedron* **2006**, *25*, 2333–2340.
[56] S. G. Zhu, D. W. Xu, S. J. Cao, J. Y. Mou, L. G. Chen, *Explos. Mater.* **2005**, *34*, 17–18.
[57] Z. H. Liu, T. L. Zhang, J. G. Zhang, S. Z. Wang, *J. Hazard. Mater.* **2008**, *154*, 832–838.
[58] Z. H. Liu, T. L. Zhang, J. G. Zhang, L. Yang, J. Zhang, Y. Zang, *Chin. J. Energ. Mater.* **2008**, *6*, 663–668.
[59] L. Yang, B. D. Wu, T. L. Zhang, Z. H. Liu, J. G. Zhang, *Propellants, Explos., Pyrotech.* **2010**, *35*, 521–528.
[60] Y. X. Ou, *Explosives*, Beijing Institute of Technology, China, **2006**.
[61] H. E. Kissinger, *Anal. Chem.* **1957**, *29*, 1702–1706.
[62] T. Ozawa, *Bull. Chem. Soc. Jpn.* **1965**, *38*, 1881–1886.
[63] Z. T. Liu, Y. L. Lao, *Initiating Explosive Experimental*, Beijing Institute of Technology, China, **1995**.
[64] G. M. Sheldrick, *SHELXS 97, Program for the Solution of Crystal Structure*, University of Göttingen, Germany, **1990**.
[65] G. M. Sheldrick, *SHELXL 97, Program for Crystal Structure Refinement from Diffraction Data*, University of Göttingen, Germany, **1997**.

Received: January 16, 2011
Published Online: April 28, 2011

